



**HAL**  
open science

## Discrete Element Modelling of a Reinforced Concrete Structure Submitted to a Rock Impact

Sébastien Hentz, Frédéric V Donzé, Laurent Daudeville

► **To cite this version:**

Sébastien Hentz, Frédéric V Donzé, Laurent Daudeville. Discrete Element Modelling of a Reinforced Concrete Structure Submitted to a Rock Impact. Italian Geotechnical Journal, 2005, 4, pp.83-94. hal-02003253

**HAL Id: hal-02003253**

**<https://hal.univ-grenoble-alpes.fr/hal-02003253>**

Submitted on 14 Feb 2019

**HAL** is a multi-disciplinary open access archive for the deposit and dissemination of scientific research documents, whether they are published or not. The documents may come from teaching and research institutions in France or abroad, or from public or private research centers.

L'archive ouverte pluridisciplinaire **HAL**, est destinée au dépôt et à la diffusion de documents scientifiques de niveau recherche, publiés ou non, émanant des établissements d'enseignement et de recherche français ou étrangers, des laboratoires publics ou privés.

# Discrete Element Modelling of a Reinforced Concrete Structure Submitted to a Rock Impact

Sébastien Hentz,\* Frédéric V. Donzé,\* Laurent Daudeville\*

## Summary

The use of a three dimensional Discrete Element Method (DEM) is proposed to study concrete submitted to rock-fall impacts. The model has already been validated through quasi-static, as well as dynamic simulations (SHPB tests). The simulation of four-point beam bending tests has validated the introduction of the reinforcement in the model. With this approach all the local parameters can be identified through a well defined procedure: thus, computations are real predictive simulations. This paper shows how rock-fall impacts have been simulated and compared with experimental results. The numerical and experimental results agree quite well both qualitatively and quantitatively, which confirms that the proposed approach can be used reliably.

*Keywords:* Discrete Element Method, reinforced concrete, rock-fall impacts, dynamic simulation, structure

## 1. Introduction

The design of concrete safety structures is a big challenge for engineers; for example some structures present in mountainous areas are dedicated to protection against natural hazards such as avalanches, rock falls, etc... and thus may be submitted to impact loads and high deformation. Despite their geometry which is usually massive, with an extremely high ratio of reinforcement, and of course a design satisfying common building standards, some are found to be totally damaged. This inconsistency demands the use of a model with high predicting abilities.

### Impact Phenomena

The response of a structure submitted to impacts depends on many parameters, but may be classified according to the following quantities:

- The relative values of both the projectile and target acoustic impedance [GERADIN & RIXEN, 1994], where this impedance is the product of the medium density by its celerity: if the projectile impedance is much higher than the target impedance, the projectile may undergo very little deformation but induces important deformation in the target, meaning penetration or perforation.

- The impact speed ranges: at low speeds (order of magnitude  $100 \text{ ms}^{-1}$ ), local phenomena are coupled with the global deformation of the structure; the characteristic durations of the loading and its associated response are typically on the order of  $1 \cdot 10^{-3} \text{ s}$ . At higher speeds (order of magnitude several hundred  $\text{ms}^{-1}$ ), the structure response becomes negligible with respect to the local behaviour in the impact zone; the loading path is usually uniaxial strain, which may induce high hydrostatic pressure, and plastic flow. The shock front is important and the structure response may be considered as discontinuous; the characteristic durations of the loading and its associated response are typically on the order of  $1 \cdot 10^{-6} \text{ s}$ . At even higher speeds (order of magnitude  $1000 \text{ ms}^{-1}$ ), the pressure may be higher than ten times the material strength and the solids may be considered as fluids.

Rock-fall impacts occur at low speeds, and as far as concrete structures are concerned, the acoustic impedances of both the impactor and the target are comparable. This means that penetration will not occur and compaction will only be very superficial. Then, the structure response may still be considered as continuous: the shock front does not need any particular treatment. But at this speed range, strain rates may reach  $1 \cdot 10^2 \text{ s}^{-1}$ , and one cannot neglect the rate effect any more. A large number of experimental results can be found in the literature (Fig. 1), in terms of the ratio dynamic strength over static strength of concrete in uniaxial tension and compression. Two distinct types of behaviour can be observed: The first one shows a linear dependence of the

\* Laboratoire Sols, Solides, Structures, Domaine Universitaire, B.P. 53, 38041 Grenoble Cedex 9 France

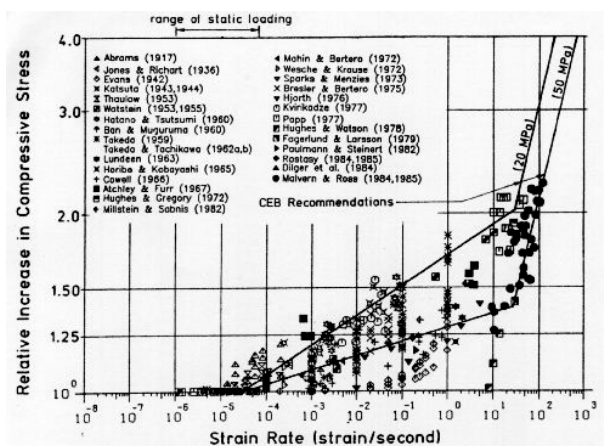


Fig. 1 – Strain rate dependency of the compressive strength, [BISCHOFF & PERRY 1991].

Fig. 1 – Resistenza a compressione uniaxiale: dipendenza dalla velocità di deformazione, [BISCHOFF & PERRY 1991].

ratio with  $\log(\dot{\epsilon})$  and is now well explained by the presence of free water in concrete, inducing an effect similar to the Stefan effect [ROSSI *et al.*, 94]. The second one is a sharp rise in the rate dependence, and is not fully understood yet. The limit between the two is around  $\dot{\epsilon} 3.10^1 s^{-1}$  in compression and around  $\dot{\epsilon} 10^0 s^{-1}$  in tension.

### Concrete modelling

Concrete has been extensively modelled, mainly by two approaches: constitutive modelling and Fracture Mechanics [LEMAITRE & CHABOCHE, 1992]. The latter considers that all non-linearities take place at the propagating crack tip and even if dynamical models exist [OH, 1990], it may not be used to describe the occurrence of a large number of discontinuities. In addition, in the frame of constitutive modelling, numerous laws are available; in particular, considering the impact speeds of interest here (which lead to few compaction and a mostly deviatoric stress state), damage and/or elasto-plastic models are mostly used. They differ in particular in the way strain rate dependency is represented.

Some authors introduce viscosity [BISCHOFF & PERRY, 1991] sometimes combined with inertia, [GARY & BAILLY, 1998]. Some micromechanics-based fracture models have led to the following type of dependence:  $\sigma_d \propto \dot{\epsilon}^n$ , where  $\sigma_d$  is the strength. It is also the case of the CEB formulation [CEB, 1993], which is one of the most comprehensive model which takes into account most of the experimental observations described in the previous section (See Fig. 1). This model will be discussed later in this paper.

When it comes to computational modelling, the first class of numerical techniques uses fixed meshes, like well-known Finite Elements/Volumes/Dif-

ferences methods. But the treatment of discontinuities with such methods demands the use of costly techniques like remeshing. The second class of techniques, the meshless methods [JOHNSON & STRYK 1989; BELYTSCHKO *et al.* 1994; MONAGHAN 1992], allows an easy modelling of discontinuities, but not of phenomena like cycles of occurrence/loss of contact, as well as crack friction. Moreover, the loss of objectivity with respect to the mesh in dynamic problems (due to the softening behaviour of all these continuous laws) has to be solved by the use of a regularization technique [BAZANT & OH, 1983; DE BORST & SLUYS, 1990; PIJAUDIER-CABOT & BENALLAL, 1993].

### 1.1. Objectives

In this paper the Discrete Element Method (DEM) [CUNDALL & STRACK, 1979], which is an alternative to continuum-type methods of increasing complexity as previously seen, is used to study structures submitted to impacts. This method does not rely upon any assumption about where and how a crack or several cracks occur and propagate, as the medium is naturally discontinuous and is very well adapted to dynamic problems.

Nevertheless, when one uses a DEM model, one has to address the issue of the modelling scale: the DEM is particularly adapted to the modelling of granular material [CUNDALL, 1989; IWASHITA & ODA, 2000; KUHN & BAGI, 2002], where one element represents one grain. Numerous authors have also used the DEM to simulate cohesive geomaterials like concrete, at the scale of the heterogeneity [POTAPOV *et al.* 1995; POTYONDY *et al.*, 1996], that is to say the size of one element is of the order of the biggest heterogeneity. This approach allows a better understanding of concrete fracture, but makes real structures modelling impossible, as the computation cost becomes “gigantic” [see LILLIU & VAN MIER, 2003] with Lattice-type models. Another approach consists in using a higher scale model, which considers that the whole assembly of elements must reproduce the macroscopic behaviour of concrete. Thus some authors like [MEGURO & HAKUNO, 1989; KUSANO *et al.*, 1992; SAWAMOTO *et al.*, 1998; CAMBORDE *et al.*, 2000] have simulated impacts on concrete structures, but usually, the model parameters are identified directly on the impact tests, and the different components of the model are not validated through reference tests.

In this paper an impact on a real 3D reinforced concrete structure has been simulated with a DE model and a quantitative comparison with experimental results is performed. Before this last step was possible, the model had to go through a validation process. First the model has been validated through quasi-static uniaxial tests, through which a param-

ter identification process could be defined [HENTZ *et al.*, 2003B;C]: thus, the modelling scale imposed by the available computing power is controlled, and the simulations are real predictive computations. Then the model validation, and in particular the reproduction of the rate effect has been extended through dynamic tests [HENTZ *et al.*, 2003a]. Last before the simulation of real structures, the introduction of the reinforcement has been validated through the simulation of beam bending tests. This paper will firstly describe the model, and then will present the structure impact results.

## 2. DEM model used

The discrete model should be able to reproduce two particular points of behaviour of concrete, with a low computation cost:

1. Common concrete behaviour is linear, elastic, isotropic and homogeneous.
2. The non-linear behaviour of concrete is closer to the behaviour of a nearly non-porous medium than to that of a granular material.

The present numerical model has been implemented within the “Spherical Discrete Element Code” [DONZÉ & MAGNIER, 1997]. It uses discrete spherical elements of individual radius and mass, which allows a quick computation of the contacts. But the orientation distribution of these has to be as homogeneous as possible to satisfy the first condition, and the assembly of elements has to be as compact as possible to satisfy the second condition. This is obtained through the use of a particular “disorder” technique, based on an algorithm described in JODREY & TORY [1985] which gives a polydisperse assembly with a particular size distribution. Once the assembly has been set, pairs of initially interacting discrete elements are identified. The interactions between these elements have been chosen to represent the elastic-brittle behaviour of concrete. To do this, elastic interaction laws with a rupture criterion are applied between two interacting elements.

Using the constitutive equations for each interaction, the numerical model solves the equations of motion. The explicit time integration of the laws of motion will provide the new displacement and velocity for each discrete element.

As time proceeds during the evolution of the system, change in the packing of discrete elements may occur and new interactions be created. One of the features of this numerical model will then be to determine the interacting neighbours of a given element. This will be achieved by defining an interaction range and identifying all elements within it which are interacting.

### 2.1. Interaction Range

The overall behaviour of a material can be reproduced by means of this model by associating a simple constitutive law to each interaction. An interaction between elements  $a$  and  $b$  of radius  $R^a$  and  $R^b$  respectively, is defined within an interaction range  $\gamma$  and does not necessarily imply that two elements are in contact. Then, these elements will interact if

$$\gamma(R^a + R^b) \geq D^{a,b} \quad (1)$$

where  $D^{a,b}$  is the distance between the centroids of elements  $a$  and  $b$  and  $\gamma=1$ . This is an important difference from classical discrete element methods which use spherical elements where only contact interactions are considered ( $\gamma=1$ ). This choice was made so that the method could simulate materials other than simple granular materials in particular those which involve a matrix as found in concretes. Moreover, it helps in modelling with DE model materials which may be considered as continuous at this scale.

### 2.2. Elastic properties

The interaction force vector  $\mathbf{F}$  which represents the action of element  $a$  on element  $b$  may be decomposed into a normal and a shear vector  $\mathbf{F}^n$  and  $\mathbf{F}^s$  respectively, which may be classically linked to relative displacements, through normal and tangential stiffnesses,  $K^n$  and  $K^s$ ,

$$\begin{cases} \mathbf{F}^n = K^n \cdot \mathbf{U}_n \\ \Delta \mathbf{F}^s = K^s \cdot \Delta \mathbf{U}_s \end{cases} \quad (2)$$

where  $\mathbf{U}_n$  is the relative normal displacement between two elements, and  $\Delta \mathbf{U}_s$  is the incremental tangential displacement. The strain energy stored in a given interaction cannot be assumed to be independent of the size of the interacting elements. Therefore interaction stiffnesses are not identical over the sample, but follow a certain distribution, which is another important particularity of the SDEC model. The macroscopic elastic properties, here Poisson's ratio  $\nu$ , and Young's modulus  $E$ , are thus considered to be the input parameters of the model.

“Macro-micro” relations are then needed to deduce the local stiffnesses from the macroscopic elastic properties and from the size of the interacting elements. Compression tests have been run with one given sample and values linking Poisson's ratio  $\nu$ , and Young's modulus  $E$  to the dimensionless values of  $K^s/K^n$  were obtained. To fit these values, relations based on the best-fit model [LIAO *et al.*, 1997] are used:

$$\left\{ \begin{array}{l} E = \frac{D_{init}^{a,b}}{\tilde{A}_{int}} K^n \frac{\alpha_1 + \alpha_2 \frac{K^s}{K^n}}{\alpha_3 + \frac{K^s}{K^n}} \\ v = \frac{1 - \frac{K^s}{K^n}}{\alpha_3 + \frac{K^s}{K^n}} \end{array} \right. \quad (3)$$

where  $D_{init}^{a,b}$  is the initial distance between two interacting elements  $a$  and  $b$ , coefficients  $\alpha_1$ ,  $\alpha_2$  and  $\alpha_3$  are the fitted values and  $\tilde{A}_{int}$  is an “interaction surface”:

$$\tilde{A}_{int} = \pi (\min(R^a, R^b))^2 \quad (4)$$

These relations are simply inverted to obtain the local stiffnesses.

### 2.3. Inelastic behaviour

#### 2.3.1. BEFORE RUPTURE

To reproduce the behaviour of geomaterials like rocks and concrete, a modified Mohr-Coulomb rupture criterion is used. Thus, for a given interaction, a maximum tensile strength  $T$  (with  $T > 0$ ) is given and defines a maximum normal force  $F_{max}^s = -T \tilde{A}_{int}$

The maximum shear force can be calculated as

$$F_{max}^s = c \tilde{A}_{int} + F^n \tan \phi_i \quad (5)$$

where  $c$  is the cohesion and  $\phi_i$  is the interparticle friction angle. If the absolute value of the shear force is  $|F^s|$ , and if it is greater than  $|F_{max}^s|$ , then the shear force is reduced to the limiting value and written as

$$F_{reduced}^s = F^s \left[ \frac{F_{max}^s}{|F^s|} \right] \quad (6)$$

Finally the model is consistent with the behaviour of concrete. Failure comes with the coalescence of micro-cracks undergoing tension.

#### 2.3.2. AFTER RUPTURE

New interactions between elements may form after the initial ones have failed, but they are not cohesive anymore: they are merely “contact” interactions, and cannot undergo any tension force. Then a classical Coulomb criterion is used, with a “contact” friction angle  $\phi_c$ . The rupture criteria used in the model is presented in Figure 2. In the initial state, the interparticle friction  $\phi_i$  takes into account the intact cemented nature of the matrix, while after

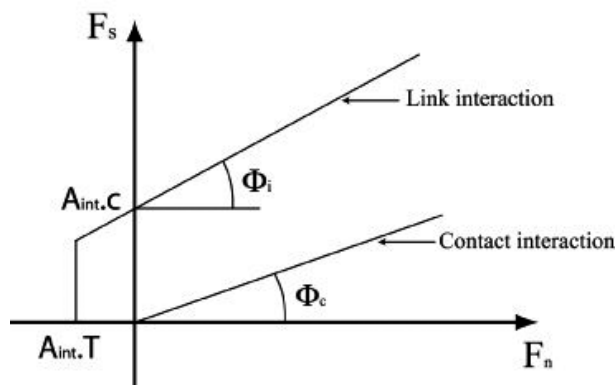


Fig. 2 – Rupture criteria used in the model.  
Fig. 2 – Criterio di rottura adottato nel modello.

failure the combined effects of the broken-up cement and the granulates are accounted for by  $\phi_c$ .

It is to be noted that the model is enriched with a local softening factor  $\beta$ , so the obtained macroscopic fracture energy can be controlled. The DE approach used considers effects at the scale of the structure and all smaller scaled energy effects which are disregarded because of computational cost are expressed by means of the softening factor.

### 2.4. Local parameters identification process

The problem is: how can a structure be modelled, in which the material and macroscopic properties (Young’s modulus, Poisson’s ratio, tensile and compressive strengths, as well as fracture energy) are known? The structure geometry is discretized with an assembly of discrete elements. Then, what value is to be given to each local parameter ( $T$ ,  $\phi_i$ ,  $\phi_c$ ,  $c$ ,  $\beta$  and  $\gamma$ ), so that the set “assembly” and “parameters” are representative of the real material, while taking into account the element size distribution, and the random aspect of the assembly generation? A procedure, fully described in HENTZ *et al.* [2003b], has been established and is based on the simulation of quasi-static uniaxial compression/traction tests:

For a standard-sized specimen:

1. A compact, polydisperse discrete element assembly is generated.
2. An elastic compression test is run with elastic local parameters given by the “macro-micro” relations (see 2.2). These relations give only a good approximation of the macroscopic elastic properties, because of the random aspect of the generation of the assembly.
3. A correction is applied according to an energy-based criterion, in relation with the characteristic size of the elements.
4. Compressive and tensile rupture axial tests are simulated to deduce the remaining local parameters.

This procedure not only allows the determination of a set of parameter values, but also ensures that the quasi-static concrete behaviour is well represented [HENTZ *et al.* 2003c]. For a large structure, it is then possible to extract a standard-sized specimen from it, and to run the procedure on this specimen. Thus, the expected properties are obtained.

### 2.5. Strain rate dependency

Compressive Split Hopkinson Pressure Bar (SHPB) tests on concrete specimens have been carried out [GARY & ZHAO, 1996; GARY, 1990] to investigate the range of high strain rates (see Fig. 1). Among these tests, three were simulated with the DE model, at different strain rates (350, 500 and 700 s<sup>-1</sup>).

The results [detailed in DONZE *et al.* 1999; HENTZ *et al.* 2003a] show that the model is able to reproduce the concrete rate effect in compression at these strain rates, and this, without requiring the use of any viscosity or any characteristic time. This result confirms the inertia-based hypothesis first proposed by BRACE & JONES [1971] and JANACH [1976]: In this range of high strain rates the material responds by bulking in the radial direction at a rate lower than the one applied, giving rise to inertial forces. The outer region of the specimen then plays a confining role, preventing the central core from unloading and thus giving the specimen a greater apparent load carrying capacity.

The conclusion is different in tension [HENTZ *et al.*, 2003a]: tensile SHPB test carried out by BRARA [1999]; KLEPACZKO & BRARA [2001] at different strain rates (36 and 108 s<sup>-1</sup>) were simulated. This time, the model has been completed with a local strain rate dependency, so the tensile rate effect, which seems to be a material-intrinsic effect at these strain rates, is well reproduced. This dependency is based on the CEB formulation: The model is modified so that the local tensile strength  $T$  depends on the strain rate  $\dot{\epsilon}$ :

$$\frac{T_{td}}{T_{ts}} = \begin{cases} 1 & \text{for } \dot{\epsilon} \leq \dot{\epsilon}_{stat} \\ \left(\frac{\dot{\epsilon}}{\dot{\epsilon}_{stat}}\right)^\delta & \text{for } \dot{\epsilon}_{stat} < \dot{\epsilon} \leq 10^0 s^{-1} \\ \theta \left(\frac{\dot{\epsilon}}{\dot{\epsilon}_{stat}}\right)^{\frac{1}{3}} & \text{for } \dot{\epsilon} > 10^0 s^{-1} \end{cases} \quad (7)$$

where  $T_{td}$  is the local dynamic tensile strength at  $\dot{\epsilon}$ ,  $T_{ts}$  is the local static tensile strength at

$$\dot{\epsilon}_{stat} = 10^{-6} s^{-1}, \log(\theta) = \left(\frac{1}{3} - \delta\right) \log(\dot{\epsilon}_{stat}), \text{ and } \delta = \frac{1}{38}$$

Considering an interacting couple of discrete elements  $a$  and  $b$ , of velocity vectors  $V_a$  and  $V_b$ , and of position vectors  $x_a$  and  $x_b$ , the discrete strain rate is given by:

$$\dot{\epsilon} = \frac{(V_b - V_a) \cdot (x_b - x_a)}{\|x_b - x_a\|^2} \quad (8)$$

### 2.6. Introduction of the reinforcement

Like MEGURO & HAKUNO [1989], MASUYA *et al.* [1994], MAGNIER & DONZÉ [1998], the reinforcement is introduced in the model as lines of elements placed next to each other. The diameter of the elements is that of the real reinforcement and the local behaviour is considered as elastic, perfectly plastic. Thus, the local parameters may be easily identified through the simulation of a tension test on the line of elements alone. This way of modelling the reinforcement is very convenient and is very well integrated in the DEM. A cross-section of the discrete setup for the simulation of a 4-point beam bending test (the dark line is the reinforcement) is shown in Figure 3; the results obtained validate the model with reinforcement.

## 3. Simulation of impacts on a real reinforced concrete structure

A rockfall gallery used to protect roads is studied. These structures are generally composed of reinforced concrete sub-structural elements (walls, columns, and foundations) and a roof slab covered by a thick backfilling layer. The roof slab is rigidly connected to sub-structural elements, and the backfilling layer is used to dissipate the impact energy; therefore, the gallery design only takes into account static dead loads (its own weight, the backfilling and rock weights): the structure is not designed to resist the impact of blocks but only to provide support for the backfilling layer. With such techniques oversized reinforced concrete elements are required. The foundations, which must be dimensioned consequently, often cause some site construction problems. Considering that the request for this type of equip-



Fig. 3 – Beam cross-section going through a reinforcement bar.

Fig. 3 – Sezione della trave in corrispondenza di una barra d'armatura.

ment will be increasing, an investigation was carried out to improve the design and limit the costs. The basic idea was to eliminate the backfilling layer and to use a semi-probabilistic approach with the notion of “acceptable damage” to the structure. For the purpose of finding an optimal solution, a new system was proposed by the French consulting company TONELLO IC, which consists in a roof slab pin supported (no continuity) on the sub-structural elements. The roof slab is subjected to the direct impact of falling rocks and slab reactions are transmitted to the sub-structures throughout ductile steel supports that act as dissipating energy fuses and protect the sub-structural elements (see Figs. 4 and 5). The slab is then designed to resist directly a falling rock impact that causes local damage limited to the shock zone. The first example of this protection system was built in 1999 at “Les Essariaux” between Albertville and Chamonix in the French Alps. The design of such a structure and its reinforcement is performed using a simplified method based on the principle of momentum and energy conservations [PERROTIN *et al.*, 2002]. Experiments were needed to validate the assumptions made along with this simplified method, and evaluate the response and the performances of this new system.

### 3.1. Experiments

The experiments consisted in dropping a concrete block from a crane above the experimental

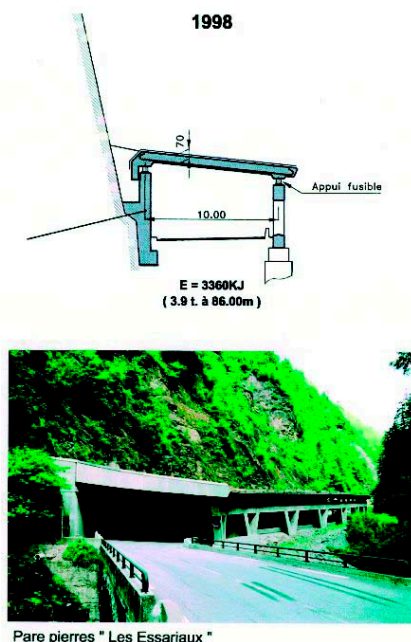


Fig. 4 – Rockfall tunnel of a new kind built in the nineties in the French Alps - Tonello IC - dossier IVOR.

Fig. 4 – Galleria artificiale paramassi del tipo introdotto nelle Alpi Francesi negli anni '90 - Tonello IC – rapporto IVOR.



Fig. 5 – Fuse - support of the slab - Tonello IC - dossier IVOR.

Fig. 5 – Supporto deformabile a perdere della piastra - Tonello IC - rapporto IVOR.

slab (see Fig. 6). The experimental slab has been designed by the TONELLO IC Company, and built by the LEON GROSSE Company. Experiments were carried out during the summer 2001 by the LOGIE (University of Chambéry). For a complete description, see MOUGIN *et al.* [2003]; DELHOMME *et al.* [2003].

**The slab:** it is a one third reduced scale model: it is 12 m long (three 4 m test zones have then been defined), 4.4 m wide, 0.28 m thick, and weighs roughly 40 t. Concrete properties are: Young's modulus  $E = 29 \text{ GPa}$ , compressive strength  $\sigma_c = 31 \text{ MPa}$ . It is densely reinforced, with longitudinal (2\*19 HA14, and 2\*16 HA20) and transversal (2\*118 HA16) reinforcement bars, as well as vertical frames (1947 HA8).



Fig. 6 – General view of the experimental setup: the impactor falling (LOGIE-ESIGEC).

Fig. 6 – Vista generale del dispositivo sperimentale (LOGIE-ESIGEC).

**The block:** it is a reinforced concrete block, a  $0.56\text{ m}$  side cube, weighing  $450\text{ kg}$ . The concrete properties are the same as for the slab.

**The fuses:** the slab lies on two lines of 11 fuses, regularly spaced every  $1.14\text{ m}$ . They consist in thin steel cylinders, which may buckle and then dissipate the shock energy. Their known properties are their stiffness ( $1.10^9\text{ N}$ ), and their critical load in compression ( $250000\text{ N}$ ).

**The tests:** three impacts were carried out: the first and the second from  $15$  and  $30\text{ m}$  high in the inner part of the slab and the third from  $30\text{ m}$  on the edge of the slab (above the support line).

**The measures:** strain gauges were placed in the slab, and displacement cells recorded the maximum deflections of the sub-surface of the slab at different positions.

### 3.2. Discrete Element Modelling

**The slab:** note that only a third of the slab has been modelled, for reasons of symmetry, and computation cost. The influence of this choice will be discussed later. The reinforcement is identical to the experimental one (see Fig. 7, 77.329 elements), and then the isotropic and polydisperse packing of “concrete” elements (110.160) is obtained through the aforementioned disorder technique around the reinforcement. Local parameters are identified with the quasi-static procedure already defined: fundamental uniaxial tests are simulated on a numerical sample extracted from the slab (see Fig. 8) so the expected concrete properties are obtained. This step is particularly important, as it ensures the predictive aspect of the computation: no parameter has been identified directly on the impact test. As for the reinforcement parameters, they have been identified with a traction test on a reinforcement bar alone.

**The block:** its geometry is as close to the experimental one as possible, the local parameters are identical to the slab ones. 10976 elements were used.

**The fuses:** they are placed at their experimental positions, and need to be very precisely defined (see

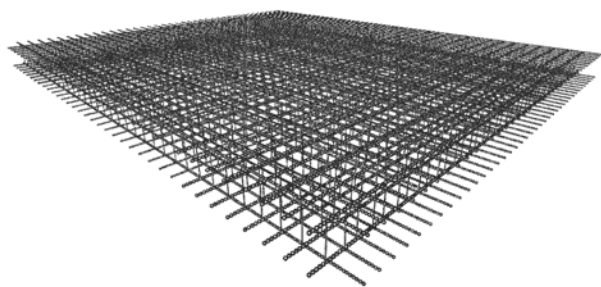


Fig. 7 – DEM modelled reinforcement.

Fig. 7 – Modello ad Elementi Distinti delle barre d'armatura.

Fig. 9). They are hollow cylinders, made of 2430 elements each. Considering the poor experimental information available concerning the fuses, a compression test has been simulated to obtain the expected stiffness and critical force. As in reality, plates have been placed between the fuses and the slab, which avoids problems due to the difference in granulometry.

Finally, 221.000 elements were used for this computation (the simulation of  $0.01\text{ s}$  real time demands roughly  $10\text{ h}$  on a P IV  $2.8\text{ GHz}$ ). Table I shows the local parameters.

**Computation conditions:** gravity is applied to the slab until equilibrium is reached prior to any computation. The block is initially placed just above the slab surface, with the initial velocity corresponding to its free fall. The impact configuration (position and orientation) has been set as close as possible to the observed experimental configuration. The block is submitted to gravity as well. Displace-

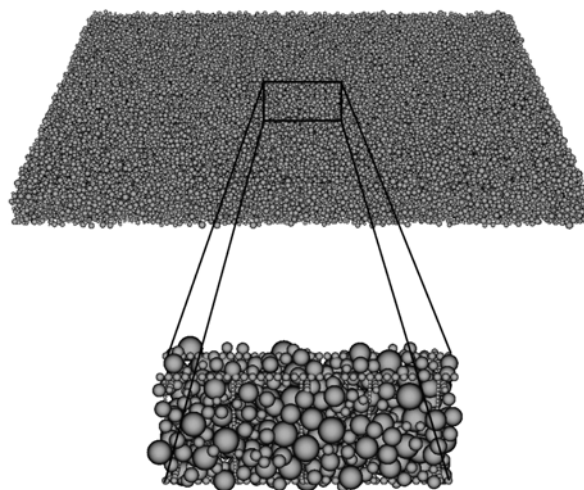


Fig. 8 – Sample extraction for the parameters identification.

Fig. 8 – Campione utilizzato per l'identificazione dei parametri.

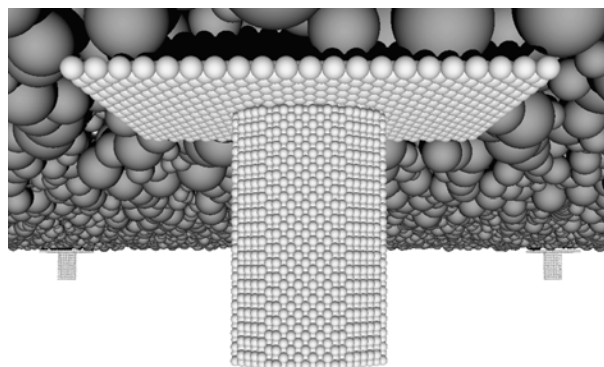


Fig. 9 – DEM model of the fuse support.

Fig. 9 – Modello ad Elementi Distinti di un supporto deformabile.

Tab. I – Local parameters used for each computation entity.

Tab. I – Parametri micromeccanici.

Parameter	concrete	steel	block	fuse
$\rho$ ( $kg.m^3$ )	2500	7800	2500	7800
g	1,4	1,05	1,4	1,05
E (GPa)	30	210	30	72
n	0,2	0,25	0,2	0,25
$\phi_i$ (degrees)	30	0	30	0
c (MPa)	3	250	6	27
T (MPa)	1,5	500	3	55
b	100	$\rightarrow \times$	100	$\rightarrow \times$
c (degrees)	30	30	30	30

ments were measured at the cells positions, on the sub-surface of the slab. The numerical setup ready for computation is shown in Figure 10.

### 3.3. Results

Table II summarizes the results obtained with the simulation of the three tests, and compares the maximum displacement obtained, and the yielding of both reinforcement and fuses. The numerical results agree quite well with experimental results with relative errors on the maximum displacements ranging from to 5 to 8 %.

As far as the centred 30 m high test is concerned, Figure 11 shows the impact force and the deflection versus time for the first 50 ms, and Figure 12 shows

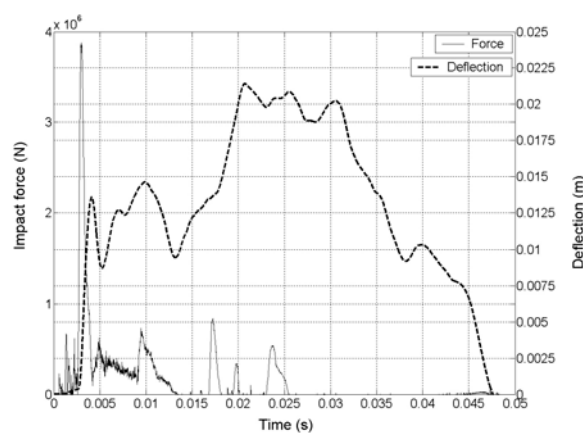


Fig. 11 – Impact force and deflection versus time.

Fig. 11 – Evoluzione temporale della forza d'impatto e della freccia.

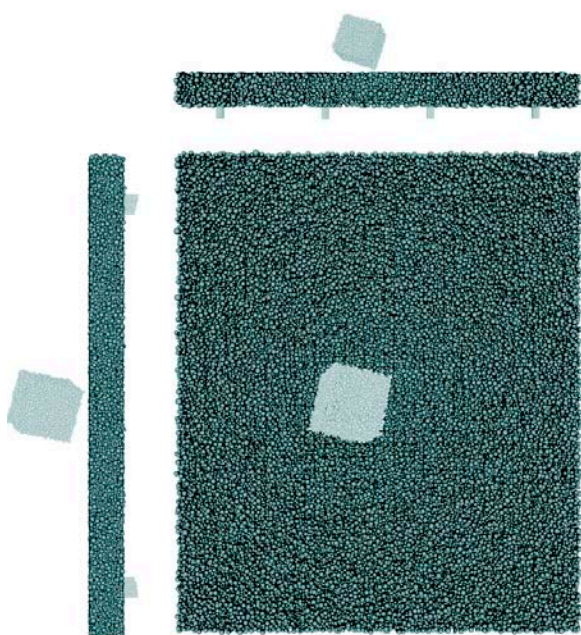


Fig. 10 – The numerical setup.

Fig. 10 – Vista generale del modello numerico.

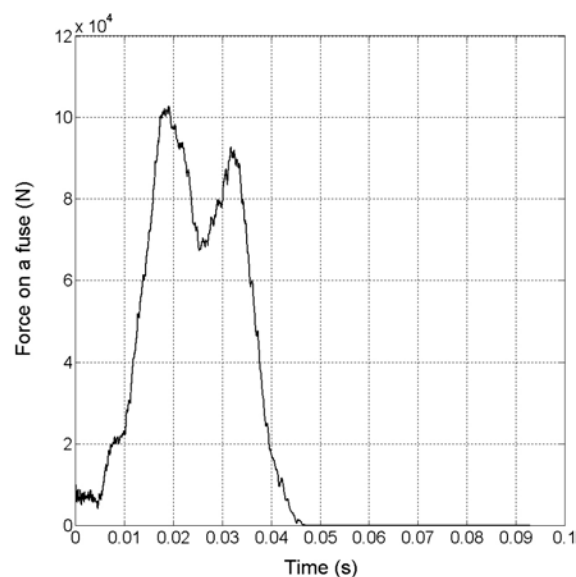


Fig. 12 – Force of the slab acting on a particular fuse versus time.

Fig. 12 – Evoluzione temporale delle azioni a livello di un elemento di supporto.

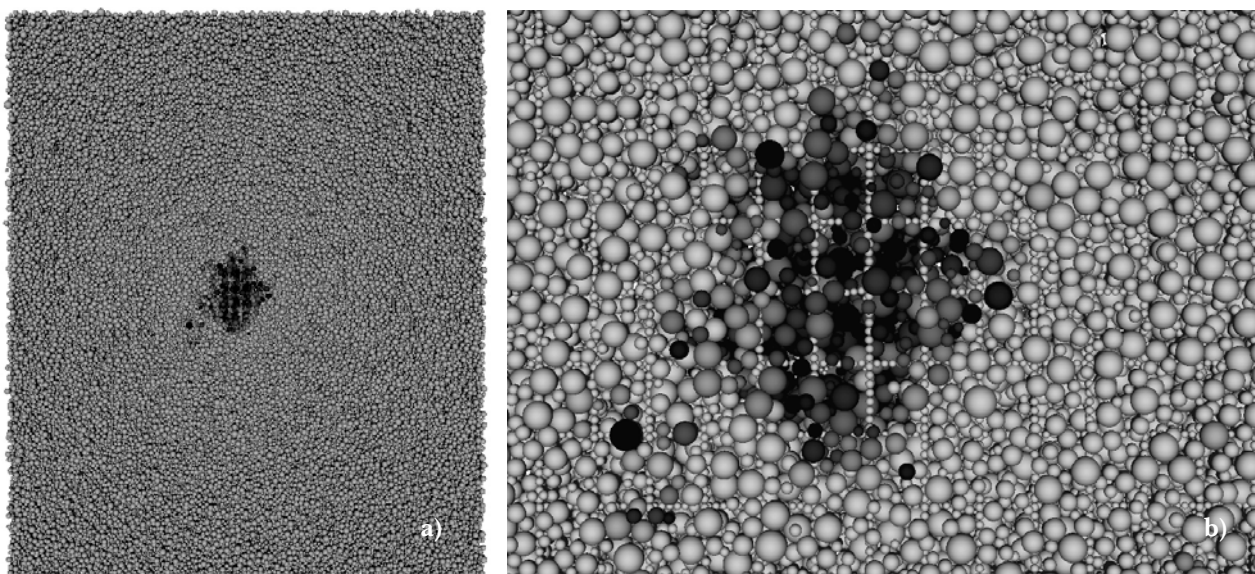


Fig. 13 – Damage of the impact face. Above view and close-up.

*Fig. 13 – Danneggiamento della piastra nella zona d'impatto (vista generale ed ingrandimento).*

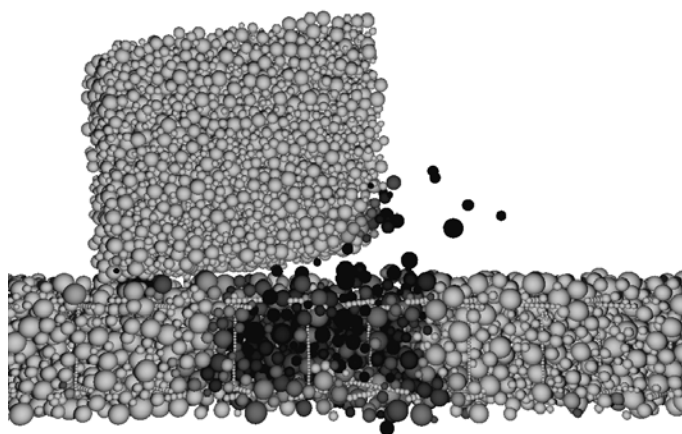


Fig. 14 – Damage of the block and the slab at  $t = 20$  ms. Cross section going through the impact point.

*Fig. 14 – Danneggiamento del blocco e della piastra ( $t = 20$  ms, sezione in corrispondenza del punto d'impatto).*

the force of the slab acting on a particular fuse. One can observe that the maximum displacement is reached in two phases: the first rise occurs right at the moment of the impact, until roughly  $4$  ms, then some fluctuation occurs, and around  $t = 13$  ms, the second rise appears. Looking at the force on the fuse, it is noticeable that during this first phase, the fuse undergoes very little effort, whereas most of the force occurs during the second phase. This means that the first phase of the deflection corresponds to a local depression of the slab, which is not coupled with the rest of the slab, whereas the second phase is due to the global movement of the slab, and is very much dependent on the boundary conditions. This second part of the displacement may then be influenced by the fact that only a third of the slab has been modelled. On the other hand, it is very likely that this impact mainly activates a simple flexion

mode, i.e. between the two lines of fuses, and then independent on the length of the slab. Moreover, the vibration frequency of the slab determined after the impact is roughly  $7.6$  Hz, close to the experimental measure,  $10$  Hz. It seems then that this modelling is representative of the real structure, and that the comparison of the maximum displacement is legitimate.

The damage of the slab impact face after the shock is shown on Figure 13, and Figure 14 shows the damage in a vertical cross-section of the slab (the damage is computed per element, and is the ratio number of broken links over the number of initial links; the darker the element, the higher the damage). Note that the damage occurs very quickly, during the local phase of the impact. At the beginning of the impact, the solicitation is mainly due to the corner of the block and the damage has a cone-

Tab. II – Comparison of numerical and experimental results.

Tab. II – Confronto tra risultati numerici e sperimentali.

Test	Experiment	Simulation
Centered 30 m high	Maximum displacement: 22,5 mm No fuse buckling No horizontal reinforcement yielding; yielding of vertical frames	Maximum displacement: 21,4 mm No fuse buckling Yielding of reinforcement
Centered 15 m high	Maximum displacement: 14,5 mm No fuse buckling No horizontal reinforcement yielding, no information on the vertical frames	Maximum displacement: 13,9 mm No fuse buckling No reinforcement yielding
30 m high on the edge	Maximum displacement: 21,5 mm Buckling of three fuses No horizontal reinforcement yielding, no information on the vertical frames	Maximum displacement: 19,9 mm Buckling of four fuses Reinforcement yielding

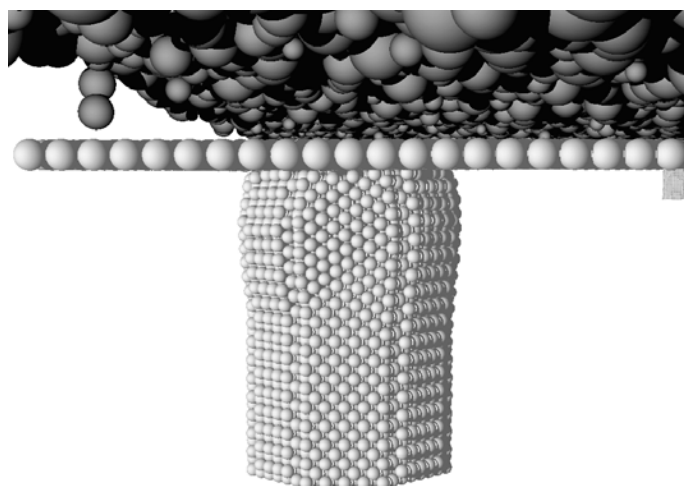


Fig. 15 – Buckled fuse.

Fig. 15 – Appoggio deformato per instabilità di parete.

like shape. The impact face is very much damaged, and locally crushed. Some spalling occurs on the sub-surface, leaving some reinforcement visible. A little part of this reinforcement has yielded.

During the 30 m high test on the edge, the three fuses closest to the position of impact have buckled. The computation has shown the same results (see Fig. 15): these three fuses have buckled, as well as a fourth one, on the opposite corner, no doubt as a result of a violent reflecting wave (the slab bounces off the fuses, and on again). This may be a limit to the fact that a third of the slab has been modelled.

#### 4. Conclusion

In previous work, a three-dimensional Discrete Element approach was proposed to study the dyna-

mic behaviour of concrete. The main specificities of this approach are the following: the modelling scale is higher than the heterogeneity scale, so the model may be used to simulate real structures, which means the DEM is mainly used here for its ability to treat discontinuities; the introduced interaction laws are then very simple and are close to macroscopic laws; last, an identification process based on quasi-static tests is used, so the quasi-static behaviour of concrete is reproduced. This identification process is the key point, as it allows predictive computations. The model validation is extended through the simulation of dynamic tests, like SHPB compressive and tensile tests: the rate effect is then taken into account. The way the reinforcement is introduced was validated through the simulation of a four-point beam-bending test.

In this work, three rock-fall tests were simulated with this model, from different heights and at different positions, on a reinforced concrete slab at a real scale. Results were compared with experimental results: Qualitatively, kinematics, damage, and fuses deformation are very coherent with respect to experimental results. Moreover, quantitatively, maximum deflections are very close to the experimental results, despite the fact that only a third of the slab has been modelled. This fact confirms that this approach may be used as a powerful predictive tool for the design of safety structures.

The Discrete Elements Method is of particular interest in the zone where damage occurs, which in the presented impact case, remains relatively small, whereas the rest of the slab remains elastic. This suggests that in this case, optimizing the discretization and/or coupling a continuous method with a discrete method would be particularly efficient in terms of computation cost. Moreover, the coupling would facilitate the computation implementation.

## References

- 1993 CEB-FIP model code (1990) – Comité Euro-international du Béton, trowbridge, Wiltshire, UK, Redwood books.
- BAZANT Z.P., OH B.H. (1983) – *Crack-band theory for fracture of concrete*. Materials and Structures 16, pp. 155-177.
- BELYTSCHKO T., LU Y.Y., GU L. (1994) – *Element-free galerkin methods*. International Journal for Numerical Methods in Engineering, 37, pp. 229-256.
- BISCHOFF P.H., PERRY S.H. (1991) – *Compressive behaviour of concrete at high strain rates*. Materials and structures, 24, pp. 425-450.
- DE BORST R., SLUYS L.J. (1990) – *Localization in a cosserat continuum under static and dynamic loading conditions*. Comp. Meth. Appl. Mech. Eng., 90, pp. 805-827.
- BRACE W.F., JONES A.H. (1971) – *Comparison of uniaxial deformation in shock and static loading of three rocks*. J. Geophys. Res., 76, pp. 4913-4921.
- BRARA A. (1999) *Etude expérimentale de la traction dynamique du béton par écaillage*. PhD Thesis, Université de Metz.
- CAMBORDE F., MARIOTTI F.C., DONZÉ F.V. (2000) – *Numerical study of rock and concrete behaviour by discrete element modelling*. Computers and Geotechnics, 27, 4, pp. 225-247.
- CUNDALL P.A. (1989) *Numerical experiments on localization in frictional materials*. ingénieur-archiv, 59, pp. 148-159.
- CUNDALL P.A., STRACK O.D.L. (1979) *A discrete numerical model for granular assemblies*. Géotechnique, 29 (1), pp. 47-65.
- DELHOMME F., MOUGIN J.P., AGBOSSOU A., MOMMESSIN M., PERROTIN P. (2003) – *Behaviour study of a rock shed slab*. In “Proceedings of the International Conference on Response of Structure to Extreme Loading”, Toronto, Canada.
- DONZÉ F.V., MAGNIER S.A. (1997) – *Spherical Discrete Element Code* In: “Discrete Element Project Report”, n. 2., GEOTOP, Université du Québec à Montréal, Canada.
- DONZÉ F.V., MAGNIER S.A., DAUDEVILLE L., MARIOTTI L., DAVENNE L. (1999) – *Study of the behaviour of concrete at high strain rate compressions by a discrete element method*. ASCE J. of Eng. Mech., 125 (10), pp. 1154-1163.
- GARY G. (1990) – *Essais à grande vitesse sur béton. Problèmes spécifiques*. Tech. Rep.. GRECO, Paris.
- GARY G., BAILLY P. (1998) – *Behaviour of quasi-brittle material at high strain rate. experiment and modelling*. European Journal of Mechanics, A/solids 17 (3), pp. 403-420.
- GARY G., ZHAO H. (1996) – *Measurements of the dynamic behaviour of concrete under impact loading*. In “Proceedings of 2nd ISIE’96”. Beijing, China.
- GERARDIN M., RIXEN D. (1994): *Mechanical Vibrations, Theory and Application to Structural Dynamics*. Wiley, Paris, 411 pp.
- GOPALARATNAM V., GERSTLE W., ISENBERG J., MINDESS S. (1996) – *State-of-the-art report on dynamic fracture*. ACI Committee, 446.
- HENTZ S., DAUDEVILLE L., DONZÉ F.-V. (2003a) – *Discrete element modelling of concrete submitted to dynamic loading at high strain rates*. Computers and Structures, 82 n. 29-30, pp. 2509-2524.
- HENTZ S., DAUDEVILLE L., DONZÉ F.-V. (2003b) – *Identification and validation of a discrete element model for concrete*. Journal of Engineering Mechanics, 130, n. 6, pp. 709-719.
- HENTZ S., DAUDEVILLE L., DONZÉ F.-V. (2003c) – *Identification of the constitutive behaviour of concrete through quasi-static discrete element simulations*. In *Constitutive Modeling of Geomaterials* (Ed. H. I. Ling, A. Anandarajah, M. T. Manzari, V. N. Kaliakin & A. Smyth), CRC Press, pp. 113.121. Boca Raton, Florida, USA.
- IWASHITA K. & ODA M. (2000) – *Micro-deformation mechanism of shear banding process based on modified distinct element method*. Powder Technology, 109, pp. 192-205.
- JANACH W., (1976) – *The role of bulking in brittle failure of rocks under rapid compression*. Inter. J. Rock Mech. Min. Sci. and Geomech, Abstr. 13, pp. 177-186.
- JODREY W.S., TORY E.M. (1985) – *Computer simulation of close random packing of equal spheres*. Physical Review A 32 (4), pp. 2347-2351.
- JONHSON G.R., STRYK R.A. (1989) – *Dynamic three-dimensional computations for solids with variable nodal connectivity for severe distortions*. International

- Journal for Numerical Methods in Engineering, 28, pp. 817-832.
- KLEPACZKO J.R. (1990) – *Dynamic Crack Initiation. Some Experimental Methods and Modelling*. Vienna New York, Springer-Verlag.
- KLEPACZKO J.R., BRARA A. (2001) – *An experimental method for dynamic tensile testing of concrete by spalling*. International journal of impact engineering, 25, pp. 387-409.
- KUHN M.R., BAGI K. (2002) – *Particle rotations in granular materials*. In 15th ASCE Engineering Mechanics Conference. ASCE, Columbia University, New-York.
- KUSANO N., AOYAGI T., AIZAWA J., UENO H., MORIKAWA H., KOBAYASHI N. (1992) – *Impulsive local damage analyses of concrete structure by the distinct element method*. Nuclear Engineering and Design, 138, pp. 105-110.
- LEMAITRE J., CHABOCHE J.-L. (1992) – *Mécanique Des Matériaux Solides*. Dunod, France.
- LIAO C.-L., CHANG T.-P., YOUNG D.-H., CHANG C.S. (1997) – *Stress-strain relationship for granular materials based on the hypothesis of best fit*. Int. J. Solids Structures, 34 (31-32), pp. 4087-4100.
- LILLIU G., VAN MIER J.G.M. (2003) – *3d lattice type fracture model for concrete*. Engineering Fracture Mechanics, 70, pp. 927-941.
- MAGNIER S.A., DONZÉ F.-V. (1998) – *Numerical simulations of impacts using a discrete element method*. Mechanics of cohesive-frictional materials, 3, pp. 257-276.
- MALVAR L.J., CRAWFORD J.E. (1998) – *Dynamic increase factors for concrete*. In 28th Department of Defense Explosives Safety Seminar, Orlando, FL.
- MASUYA H., KAJIKAWA Y., NAKATA Y. (1994) – *Application of the distinct element method to the analysis of the concrete members under impact*. Nuclear Engineering and Design, 150, pp. 367-377.
- MAZARS J. (1984) – *Application de la mécanique de l'endommagement au comportement non linéaire et à la rupture du béton de structure*. Master's Thesis, Université Paris VI.
- MEGURO K., HAKUNO M. (1989) – *Fracture analyses of concrete structures by the modified distinct element method*. Structural Engineering/Earthquake Engineering, 6 (2), pp. 283-294.
- MONAGHAN J.J. (1992) – *Smoothed Particle Hydrodynamics*. Ann. Rev. Astron and Astrophysics.
- MOUGIN J.-P., PERROTIN P., MOMMESSIN M., TONELLO J., AGBOSSOU A. (2005) – *Rock fall impact on reinforced concrete slab: An experimental approach*. International Journal of Impact Engineering, 31, pp. 169-183.
- OH B.H. (1990) – *Fracture behaviour of concrete under high rates of loading*. Engineering Fracture Mechanics, 35 (1/2/3), pp. 327-332.
- PERROTIN P., MOMMESSIN M., MOUGIN J.-P., TONELLO J. (2002) – *Etude expérimentale du comportement d'une dalle pare-blocs*. Revue Française de génie civil, 6, 5/2002, pp. 723-734.
- PIJAUDIER-CABOT G., BENALLAL A. (1993) – *Strain localization and bifurcation in a nonlocal continuum*. International Journal of Solids and Structures, 30 (13), pp. 1761-1775.
- POTAPOV A.A., HOPKINS M.A., CAMPBELL C.S. (1995) – *A two-dimensional dynamic simulation of solid fracture part I: Description of the model*. International Journal of Modern Physics, 6 (3), pp. 371-398.
- POTYONDY D.O., CUNDALL P.A., LEE C.A. (1996) – *Modelling rock using bonded assemblies of circular particles*. Rock Mechanics, pp. 1937-1944.
- ROSSI P., VAN MIER J.G.M., TOUTLEMONDE F., LE MAOU F., BOULAY C. (1994) – *Effect of loading rate on the strength of concrete subjected to uniaxial tension*. Materials and Structures, 27, pp. 260-264.
- SAWAMOTO Y., TSUBOTA H., KASAI Y., KOSHIBA N., MORIKAWA H. (1998) – *Analytical studies on local damage to reinforced concrete structures under impact loading by discrete element method*. Nuclear Engineering and Design, 179, pp. 157-177.

## Impatto di blocchi rocciosi su di una struttura in calcestruzzo armato: modellazione ad Elementi Distinti

### Sommario

L'articolo propone l'utilizzo di un programma tridimensionale ad Elementi Distinti per lo studio di strutture di protezione contro la caduta massi in C.A. La capacità del modello nel riprodurre il comportamento meccanico del calcestruzzo è stata preventivamente testata sia in campo statico che in campo dinamico (prove SHPB). L'utilizzo del modello stesso è stato quindi validato per strutture rinforzate, facendo riferimento ad una prova di flessione APB su di una trave in C.A. È inoltre stata messa a punto una procedura ben definita per la calibrazione dei parametri micromeccanici. Si presenta l'applicazione del modello alla simulazione di impatti di blocchi su una lastra di copertura di una galleria artificiale. Il buon accordo tra i dati sperimentali disponibili e i risultati della simulazione numerica mostrano l'affidabilità del modello per questo tipo di applicazione.